Science of the Total Environment 723 (2020) 138080

Contents lists available at ScienceDirect

Science of the Total Environment

journal homepage: www.elsevier.com/locate/scitotenv

Stimulation of methane production from benzoate with addition of carbon materials

Fang Zhang [a], Ding-Kang Qian [a], Xian-Bin Wang [b], Kun Dai [a], Ting Wang [b], Wei Zhang [b], Raymond Jianxiong Zeng [a,b,*]

[a] Center of Wastewater Resource Recovery, College of Resources and Environment, Fujian Agriculture and Forestry University, Fuzhou, Fujian 350002, China
[b] CAS Key Laboratory of Urban Pollutant Conversion, Department of Chemistry, University of Science and Technology of China, Hefei, Anhui 230026, People's Republic of China

HIGHLIGHTS

- Conductive carbon materials can stimulate methanogenic degradation of benzoate.
- The sequence of promoting benzoate degrading is GAC > MwCNTs ~ Graphite > Control.
- 82–93% of the electrons released from benzoate are finally recovered as methane.
- Pathways involved bacteria of *Syntrophus*, methanogens, and DIET are proposed.
- Acetate is detected as the main intermediate of benzoate, while H_2 is undetected.

GRAPHICAL ABSTRACT

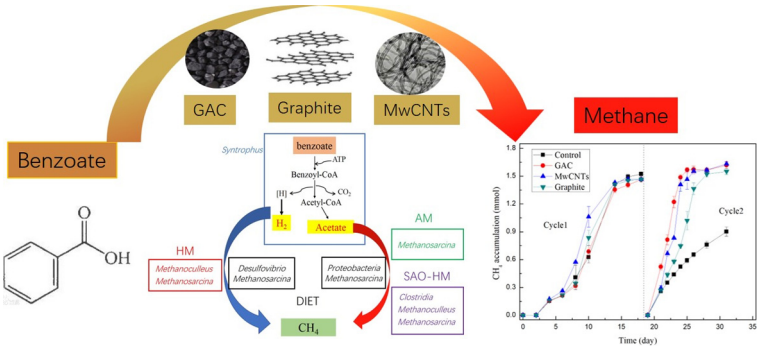

ARTICLE INFO

Article history:
Received 9 January 2020
Received in revised form 18 March 2020
Accepted 18 March 2020
Available online 19 March 2020

Editor: Yifeng Zhang

Keywords:
Benzoate
Carbon materials
Syntrophus
Acetoclastic methanogens
Hydrogenotrophic methanogens
Direct interspecies electron transfer

ABSTRACT

Huge amounts of wastewater that contain aromatic compounds such as benzene and phenols are discharged worldwide. Benzoate is a typical intermediate in the anaerobic transformation of those aromatic compounds. In this study, electrically conductive carbon-based materials of granulated activated carbon (GAC), multiwalled carbon nanotubes (MwCNTs), and graphite were evaluated for the ability to promote the benzoate degradation. The results showed that 82–93% of the electrons were recovered in CH_4 production from benzoate. The carbon materials stimulated benzoate degradation in the sequence of GAC (5 g/L) > MwCNTs (1 g/L) ~ Graphite (0.1 g/L) > Control. Acetate was the only detected intermediate in the process of benzoate degradation. Taxonomic analyses revealed that benzoate was degraded by *Syntrophus* to acetate and H_2, which were subsequently converted to methane by *Methanosarcina* (both acetoclastic methanogens and hydrogenotrophic methanogens) and *Methanoculleus* (hydrogenotrophic methanogens), and direct interspecies electron transfer (DIET) of *Desulfovibrio* and *Methanosarcina*. Thus, these results suggest a method to effectively enhance the removal of aromatic compounds and methane recovery.

* Corresponding author at: Center of Wastewater Resource Recovery, College of Resources and Environment, Fujian Agriculture and Forestry University, Fuzhou, Fujian 350002, China.
E-mail address: rzeng@ustc.edu.cn (R.J. Zeng).

https://doi.org/10.1016/j.scitotenv.2020.138080
0048-9697/

1. Introduction

Many effluents that contain aromatic compounds of benzene, toluene, and phenols are discharged from petroleum refining, production of resins and plastics, leather and textile manufacturing, chemical and petrochemical plants, and the pharmaceutical industry (Pathiraja et al., 2019; Singh et al., 2017; Venkidusamy et al., 2016). There is growing awareness that these compounds have properties of toxicity, mutagenicity, and carcinogenicity, and are resistant to biodegradation (Mrozik and Piotrowska-Seget, 2010). Under anaerobic conditions, benzoate is detected as a typical intermediate in the anaerobic transformation of those aromatic compounds (Fuchs et al., 2011; Ghattas et al., 2017). For this reason, the development of improved methods for the efficient degradation of benzoate under anaerobic conditions is an important strategy to remove those aromatic compounds.

However, the benzoate degradation to H_2 and acetate under anaerobic conditions is thermodynamically unfavorable (Table 1) (Morris et al., 2013). For example, when the partial pressure of H_2 (P_{H2}) decreases from 1 atm to 10 Pa, the Gibbs free energy in Eq. (1) decreases from 86.3 to 17.4 kJ/mol. Thus, methanogens of acetoclastic methanogenesis (Eq. (2)) and hydrogenotrophic methanogenesis (Eq. (3)) are required to consume the intermediate products of H_2 and acetate. Especially, the interspecies electron transfer via H_2 is thought to be the main mechanism of syntrophic methanogenesis (Morris et al., 2013). Anaerobic digestion (AD) does not require sterilization, can be applied in continuous fermentation, is adaptive to changes in feedstock or operation conditions, and is suitable for benzoate conversion (Eq. (4)) (Dai et al., 2017; Tabassum et al., 2017). Upadhyay et al. (2008) analyzed benzoate degradation by mixed culture fermentation and found higher rates of benzoate degradation than of phenol, but the high concentration of benzoate (11.7 g-COD/L) also notably inhibited bacterial activity. Adding electron acceptors such as SO_4^{2-} also can stimulate the degradation of benzoate, for example, Guo et al. (2015) reported that the activated sludge could remove phenol (>90%) in an up-flow anaerobic sludge blanket (UASB) reactor. Aburto-Medina and Ball (2015) enriched benzoate-degrading bacteria and found that hyper-thermophilic archaeon of *Ferroglobus placidus* and *Geobacter strains Ben* and *metallireducens* could anaerobically degrade benzene in a process coupled to the reduction of Fe(III).

Zhuang et al. (2015) reported the methanogenic rates in benzoate degradation were enhanced in the presence of hematite (25%) and magnetite (53%), which was due to direct interspecies electron transfer (DIET) mediated methanogenesis. However, the specific bacterial species responsible for benzoate degradation was not identified and the overall benzoate-degrading process was not clearly described. Recently, the process of DIET, in which two or more microbes exchange electrons through microbial pili or conductive solids, has been carried out as an alternative mechanism to enhance the methanogenic degradation of organic matter (Jin et al., 2019; Shrestha and Rotaru, 2014). This novel strategy has been tested in a methanogenic wastewater digester and in co-culture of *Geobacter* spp. and methanogens (i.e., *Methanosarcina barker*i and *Methanosaeta harundinacea*) (Morita et al., 2011; Rotaru et al., 2014). Both the conductive carbon materials and minerals, including granulated activated carbon (GAC), multiwalled carbon nanotubes (MwCNTs), graphite, biochar and even Nano-Fe_3O_4 particles, have been demonstrated to stimulate DIET-mediated methanogenesis (Martins et al., 2018; Salvador et al., 2017; Xiao et al., 2018). In this process, the presence of carbon-based materials also stimulates stable microorganism community structure and serves as the conductors to transfer extracellular electrons (Li et al., 2019; Liu et al., 2017). Meanwhile, Salvador et al. (2017) highlighted the additional role of MwCNTs during butyrate degrading as an available surface for microorganism's attachment and nutrients adsorption. Li et al. (2018) reported that adding the conductive carbon cloth in wetland soil can be benefit to acetoclastic methanogenesis instead of CO_2 reduction. Thus, besides DIET, conductive materials provided much more roles in AD. However, the details of this mechanism have not been determined in the benzoate degrading process. In particular, the molecular methods such as Illumina high-throughput sequencing are required to identify the dominant bacteria in DIET to explain the effects on reactor performance and the benzoate degrading mechanism (Salvador et al., 2017; Varjani, 2017).

To the best of knowledge, there have been no studies of the stimulation of methane production from benzoate by the addition of carbon materials. Consequently, the aims of this study were i) to assess the possibility of different conductive carbon materials (GAC, MwCNTs, and graphite) to promote the benzoate degradation and methane production; ii) to analyze the intermediates in the benzoate-degrading process; iii) to identify enriched bacteria using Illumina MiSeq high-throughput sequencing; iv) to demonstrate the mechanism that the enriched bacteria stimulate the benzoate-degrading process. Thus, these results could be exploited to enhance methane from the recalcitrant aromatic hydrocarbons.

2. Materials and methods

2.1. Anaerobic incubation and pretreatment of carbon materials

The inoculum was collected from a laboratory-scale mesophilic anaerobic digester (Zhang et al., 2018). 2 mM benzoate, 50 mL sludge, and 150 mL mineral medium were added in a 250 mL anaerobic reactor (R1) of to enrich benzoate-degrading bacteria. The mineral medium was the same as that of Dai et al. (2019). GAC (12–20 mesh with the outside diameter (OD) of 0.9–1.7 mm, Sigma-Aldrich) was soaked with 1 M acid and 1 M alkali solution four times to remove any impurities, and then was rinsed with deionized water until reaching pH of 7.0. A sample of 2 g of MwCNTs (L-MWNT-4060 with OD of 40–60 nm, Shenzhen Nanotech Port Co., Ltd) was evenly dispersed in 100 mL deionized water by ultrasound for 30 min. The basic parameters of the graphite used here (Chengdu Organic Chemistry Co., Ltd.) are reduced graphene oxide, purity > 98 wt %, layers < 10, diameter 0.5–3 μm, thickness 0.55–3.74 μm, and specific surface area 500–1000 m^2/g.

Table 1
Gibbs free energy of bioreactions in benzoate degrading process.

Bioreactions[a]	ΔG^b (kJ/mol)	ΔG^c (kJ/mol)	ΔG^d (kJ/mol)
$C_7H_5O_2^- + 6H_2O \rightarrow 3CH_3COO^- + CO_2 + 3H_2 + 2H^+$ (1)	86.3	29.7	17.4
$CH_3COOH \rightarrow CH_4 + CO_2$ (2)	−35.7	−35.7	−35.7
$4H_2 + CO_2 \rightarrow CH_4 + 2H_2O$ (3)	−130.7	43.1	79.9
$C_7H_5O_2^- + H^+ + \frac{9}{2}H_2O \rightarrow \frac{15}{4}CH_4 + \frac{13}{4}CO_2$ (4)	−118.8	−118.8	−118.8

[a] Bioreactions were collected from Morris et al. (2013) and Zhuang et al. (2015).
[b] Calculated under standard conditions except pH of 7.0.
[c] Calculated under standard conditions except P_{H2} 50 Pa and pH 7.0.
[d] Calculated under standard conditions except P_{H2} 10 Pa and pH 7.0.

2.2. Experimental design

The experiments to determine methane production from benzoate included four groups (Table 2). To lower the adsorption of benzoate by GAC, 5 g/L was used in this study. And due to the toxicity of MwCNTs and Graphite on anaerobic bacteria, lower concentrations of 1.0 g/L MwCNTs (Salvador et al., 2017) and 0.1 g/L Graphite (Xiao et al. (2019) were applied in this study. Consequently, in the control group, no carbon materials were added, and for the groups of GAC, MwCNTs, and Graphite, 0.25 g granular activated carbon, 2.5 mL multi-walled carbon nanotube solution, and 5 mg graphite were added into the serum bottles of 120 mL (50 mL working volume), respectively. All experiments were conducted in triplicate ($n = 3$). In an anaerobic glove box, R1 sludge of 100 mL was taken and the supernatant was removed by centrifugation at 8000*g* for 5 min. The centrifuged sludge was re-suspended in 10 mL fresh culture medium, and then 0.5 mL solution was taken and transferred to each of 12 serum bottles as the inocula. Fresh medium and 0.5 mM sodium benzoate were also added into these serum bottles to reach a total working volume of 50 mL. The 12 serum bottles were sparged with N_2 (>99.99%) for 20 min and then were tightly sealed. Finally, these bottles were incubated at a constant temperature of 37 °C.

2.3. Analytical methods

The produced gas was sampled with a high-pressure injection needle (SGE, Australia). The gas (H_2, CH_4, and CO_2) contents and concentrations of volatile fatty acids and ethanol were determined by gas chromatograph methods, and the detailed methods were described by Zhang et al. (2015). Benzoate concentration was determined by an Agilent HPLC (Agilent 1260 infinity) using the method of Zhuang et al. (2015).

2.4. The degrading rate of benzoate

The first-order kinetic model was used to calculate the benzoate degrading rate (k, 1/h) according to Eq. (5) (Zhuang et al., 2015), in which, C_0 (mmol/L) and C_t (mmol/L) represent the benzoate concentrations at days 0 and t, respectively; t represents the degrading time, in days.

$$\ln\left(\frac{C_t}{C_0}\right) = -kt \tag{5}$$

2.5. Microbial morphology

The microbial morphology of different electrically conductive materials was observed by scanning electron microscopy (SEM; SIRION200, FEI, USA) according to the method of Wang et al. (2018).

2.6. Microbial community analysis

DNA samples were extracted on day 33 from the serum bottles of four groups of Control, GAC, CNTs, and Graphite using a PowerSoil™ DNA Isolation Kit. Four DNA samples were amplified using PCR primers 515F-806R. Sequencing was then carried out by Majorbio Corporation. The sequencing data for the raw sludge and enriched sludge samples from the Control, GAC, CNTs, and Graphite groups were archived in the NCBI Sequence Read Archive with accession numbers of SRR SRR5439691, SRR7285287, SRR7285288, SRR7285289, and SRR7285290, respectively.

Table 2
Experimental conditions of four groups for benzoate degradation.

Group name	Control	GAC	M_WCNTs	Graphite
Concentration of Carbon material	–	5 g/L	1 g/L (2.5 mL solution)	100 mg/L
Inocula volume (mL)	0.5	0.5	0.5	0.5
Medium volume (mL)	49	49	46.5	49
Substrate volume (mL)	0.5	0.5	0.5	0.5

3. Results and discussion

3.1. Benzoate degradation and CH_4 production for cultures with added carbon materials

To measure the initial benzoate-degrading activity of inoculum, 10 mM benzoate or 10 mM acetate was utilized as the substrate (Fig. S1). In the control experiment with added acetate, methane was detected at the first day and acetate was totally consumed after 17 days. However, in the experiment with benzoate, benzoate was not consumed by AD within 20 days, likely due to its toxicity. At day 32, little methane (4.5 ± 1.0%, $n = 3$) was detected. The cultivation was then extended to 100 days to enrich benzoate-degrading bacteria.

Fig. 1 shows benzoate degradation in the presence of GAC, MwCNTs and graphite. Due to benzoate adsorption on GAC, the initial measured benzoate concentration (8.70 ± 0.11 mmol/L, n = 3) in the GAC group was lower than that of the other three groups (9.51 ± 0.08 mmol/L, $n = 9$). After 14 days in Cycle 1, the benzoate was all totally consumed in four groups. The benzoate concentrations at days 0 and 10 were used to calculate benzoate-degrading rates by first order kinetic fitting (Fig. S2); the *k* value in the GAC group (0.184 1/h) was higher than the values for the MwCNTs (0.120 1/h), Graphite (0.084 1/h), and the Control (0.077 1/h) groups. After benzoate was totally consumed in Cycle 1, 10 mmol/L of benzoate was added again, and N_2 was used to remove biogas in the headspace. In Cycle 2, the benzoate-degrading rates increased notably. In the GAC group, benzoate was totally consumed within 4 days and the degrading rate was 0.51 1/h, higher than that of Graphite (0.404 1/h), MwCNTs (0.383 1/h), and Control (0.266 1/h) groups. Zhuang et al. (2015) reported that adding hematite and magnetite increased the benzoate degradation rates by 16% and 39%, respectively. In this work, GAC addition resulted in an increase of over 91% vs the Control group. The carbon materials stimulated benzoate degradation according to the sequence of GAC (5 g/L) > MwCNTs (1 g/L) ~ Graphite (100 mg/L) > Control.

Methane is the final metabolite of methanogenesis in AD, and Fig. 2 shows the accumulation of methane for two cycles of benzoate degradation. The methane yields did not increase after 16 days in Cycle 1, with similar final methane yields in the four groups, around 1.5 mmol (Control, 1.52 ± 0.02 mmol; GAC, 1.46 ± 0.02 mmol; MwCNTs, 1.47 ± 0.02 mmol; Graphite, 1.47 ± 0.01 mmol). Thus, the adsorption of benzoate on GAC could be ignored for methane production. In Cycle 2, the methane yield in the Control group decreased to 0.90 ± 0.05 mmol, which was lower than that in Cycle 1. The final methane yields in GAC, MwCNTs, and Graphite did not change much and were 1.62 ± 0.04, 1.63 ± 0.02, and 1.55 ± 0.03 mmol, respectively. The methane yield on day 25 was 0.59, 1.57, 1.46, and 1.02 mmol/L in the Control, GAC, MwCNTs, and Graphite groups, respectively, which meant that carbon materials stimulated benzoate degradation according to the sequence of GAC (5 g/L) > MwCNTs (1 g/L) > Graphite (100 mg/L) in Cycle 2.

Next, the electron balance was calculated based on CH_4 and CO_2 production from benzoate according to Eq. (4), and Fig. 3 shows the calculated electron recovery in benzoate degradation in cycles 1 and 2. In the Control group in Cycle 1, the percentage of electron balance was 85%, and it ranged from 82%–96% in GAC, MwCNTs, and Graphite groups. The electron percentage of substrate to biomass in AD is generally around 10% (Zhang et al., 2014). Thus, good electron balances were achieved in these experiments, indicating that methanogenesis was the predominant electron acceptor in these experiments. In contrast,

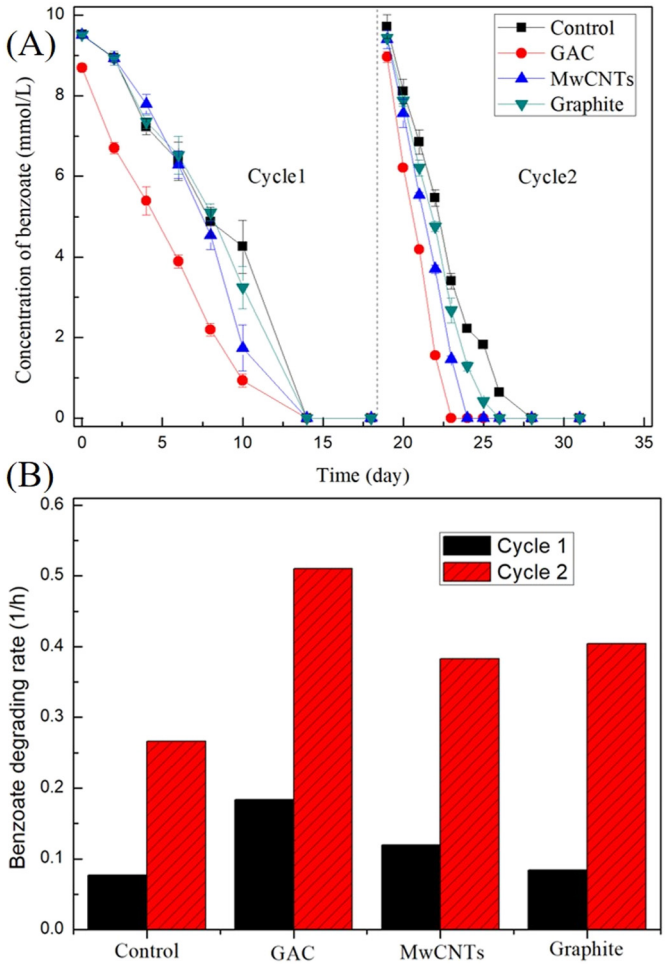

Fig. 1. Profiles of benzoate degradation with the addition of carbon materials: (A) benzoate concentration vs time (B) benzoate degrading rates by first-order kinetic equation.

for the Control group in Cycle 2, the percentage of electron balance was only 49%, indicating that in addition to CH_4, other metabolites such as acetate may accumulate in benzoate degradation (Zhuang et al., 2015).

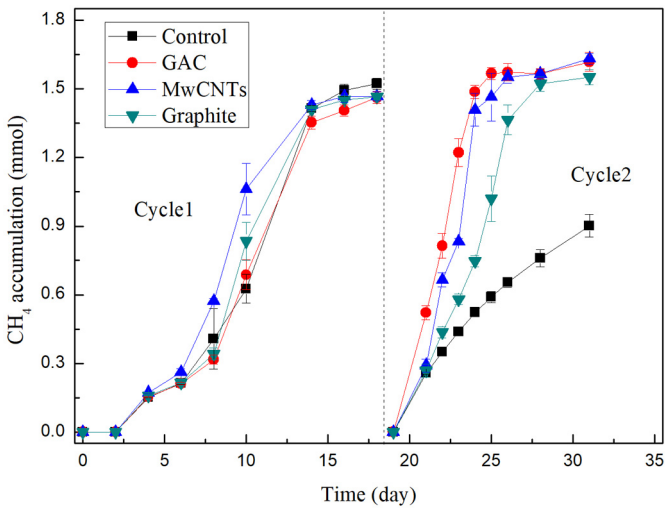

Fig. 2. The accumulation of CH_4 in two cycles of benzoate degradation.

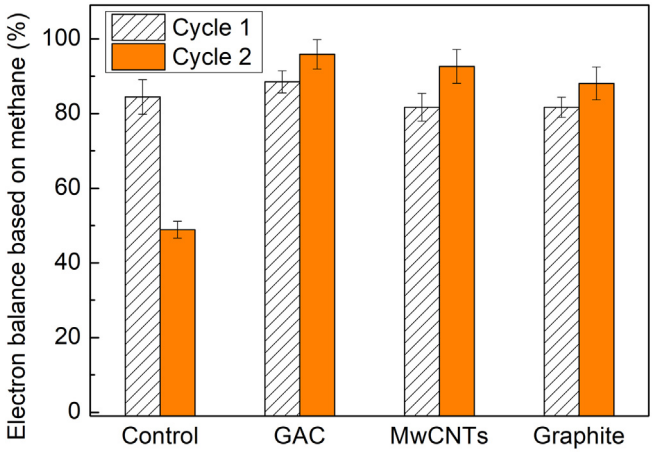

Fig. 3. Electron recovery of CH_4 in benzoate degradation at the end of each cycle.

3.2. Production of intermediates in benzoate degradation

The intermediates, including acetate, formate, butyrate, and H_2, are detected in anaerobic degradation of benzoate to CH_4 (Fuchs et al., 2011; Nobu et al., 2017; Vogt et al., 2011), but in this study, formate, butyrate, and H_2 were not detected throughout the cycle, and acetate was the only metabolite detected in the liquid. Fig. 4 shows acetate accumulation in the benzoate-degrading process. In Cycle 1, the maximum concentrations of acetate on day 8 in the Control, GAC, MwCNTs, and Graphite groups were 12.6 ± 0.9, 16.3 ± 2.0, 8.8 ± 1.3 and 10.8 ± 0.7 mM, respectively. The acetate was totally consumed by methanogens on day 16. In Cycle 2, the maximum concentration acetate in GAC, MwCNTs, and Graphite groups reached 9.1 ± 1.6 (day 22), 12.7 ± 3.0 (day 23), and 16.7 ± 1.5 (day 24) mM, respectively. Acetate was undetected in GAC, MwCNTs, and Graphite groups after day 27. Thus, good electron balance in GAC, MwCNTs, and Graphite groups was achieved when considering the CH_4 yields.

The maximum acetate concentration in the Control group was 28.7 ± 0.8 mM on day 28, much higher than the concentration of other groups. The acetate was not totally consumed even after day 33, which resulted in low electron balance (49%) when considering only the CH_4 yields. After considering the acetate yield, the electron balance in the Control group increased to 86%. The carbon mass recovery ranged from 95% to 107% in four groups (Table S1), which meant that acetate

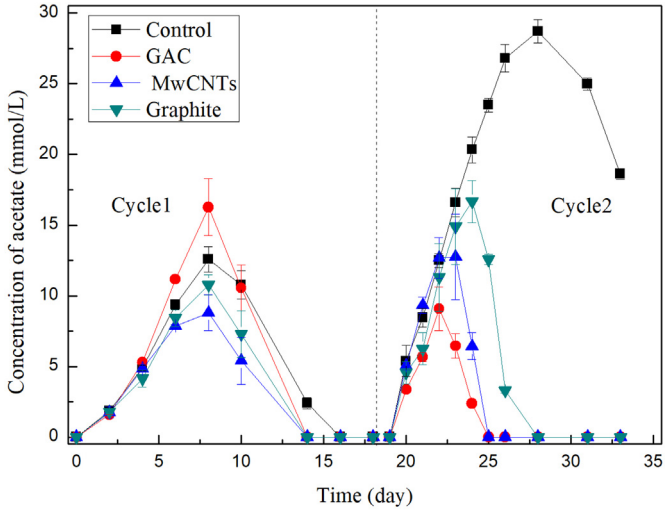

Fig. 4. Acetate accumulation during benzoate degradation.

was the main intermediate. The produced acetate was further converted to CH_4 and CO_2 by methanogens. Addition of GAC, MwCNTs, or Graphite did not change the degrading pathway of benzoate.

Due to thermodynamic barrier under methanogenic conditions, acetate can be the only metabolite in the oxidation of benzoate when H_2 is totally consumed (Fuchs et al., 2011; Zhuang et al., 2015). Similarly, after selective enrichment of hydrogenotrophic methanogens (>90%), Chen et al. (2016) also reported primary production of acetate (>90%) from tofu wastewater with no hydrogen generation in extreme-thermophilic mixed culture fermentation. In this study, the rates of benzoate degradation, CH_4 generation, and acetate production and consumption were all higher in the presence of GAC, MwCNTs, or Graphite than without addition of carbon materials (Figs. 1, 2, and 4). Thus, the carbon materials of GAC, MwCNTs, or Graphite stimulated the syntrophic degradation of benzoate.

3.3. Analysis of microbial community and benzoate degradation

SEM analysis revealed that rod and coccoid shape bacteria dominated the benzoate-degrading bacteria (Fig. S3). To more fully determine the diversities of microbial community, DNA samples were prepared from the Control, GAC, MwCNTs, and Graphite groups and subjected to Illumina high-throughput sequencing. Over 60,000 effective sequences were obtained for each sample. High coverages of all above 0.9990 in four groups were obtained. Table 3 shows the sequencing indices. The OTU number in the Control group was 213. After the addition of carbon materials, the values did not change much after day 33 in Cycle 2, and were 220 (GAC), 198 (MwCNTs), and 211 (Graphite) for the three groups. The curves of rarefaction and Shannon index (Fig. S4) showed that the sequencing depth met the demand to analyze the enriched consortium.

Sequencing analysis of the raw sludge (Fig. S5) was the same as that reported by Zhang et al. (2018), with the percentages of bacteria and archaea at the domain level of 50.65% and 49.35%, respectively (Fig. S5A). At the phylum level (Fig. S5B), Euryarchaeota was the only detected archaea, 49.35%, and the main detected bacteria included Firmicutes (21.91%), Proteobacteria (7.22%), and Bacteroidetes (5.59%). Moreover, at the genus level (Fig. S5C), *Methanosaeta* (39.38%, acetoclastic methanogen) was the main archaea, with low percentages of *Methanobacterium* (5.96%, hydrogenotrophic methanogen) and *Methanoculleus* (2.96%, hydrogenotrophic methanogen). Family_XIV_uncultured (10.08%), *Atribacteria*_norank (4.43%), and *Gelria* (4.39%) were the three main bacterial groups.

After benzoate addition, the microbial community changed notably (Fig. 5A). In the group of control, the percentage of Euryarchaeota at the phylum level decreased to just 0.13%. The low archaeal percentage was expected due to the toxicity of benzoate (Upadhyay et al., 2008). Analysis of bacterial diversity revealed the percentages of Proteobacteria and Bacteroidetes of 61.12% and 12.16%, respectively. Other bacteria were present at low percentages, such as Cloacimonetes (8.19%), Synergistetes (5.90%), and Spirochaetae (5.76%).

Dosing carbon materials did not significantly change microbial community. At the phylum level, in the GAC, MwCNTs, and Graphite group samples, the percentages of Euryarchaeota were 0.12%, 0.15%, and 0.16%, respectively, which were similar to that of the Control group (0.13%). Proteobacteria and Bacteroidetes were the two main enriched bacteria. In the groups of GAC and MwCNTs, their percentages did not change notably from that of the Control group, with 60.69% and 8.43%, and 61.20% and 11.05%, respectively. In the Graphite group, the percentage of Proteobacteria decreased to 52.20%, but the percentage of Bacteroidetes was stable at 11.60%.

Table 3
General indices of benzoate degrading bacteria by Illumina high-throughput sequencing technology.

Samples	OTU	ACE	Chao1	Simpson	Shannon	Coverage
Control	213	215.6	214.9	0.0804	3.1118	0.9999
GAC	220	226.2	225.8	0.0878	3.0238	0.9998
MwCNTs	198	200.6	200.3	0.1327	2.7936	0.9999
Graphite	211	213.5	212.4	0.0832	3.1076	0.9999

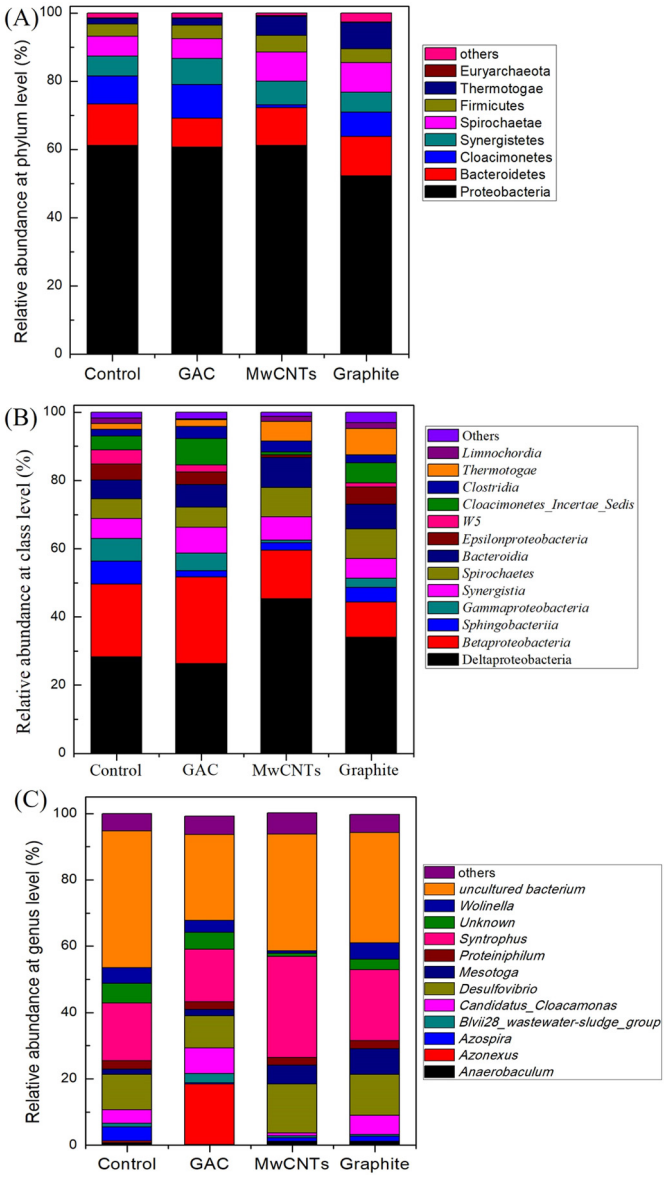

Fig. 5. Taxonomic classification of the benzoate degrading bacteria at the levels of phylum (A), class (B) and genus (C) by Illumina high-throughput sequencing. Taxonomic groups accounting for <1% are classified in the artificial group "others".

Fig. 5B shows the taxonomic characteristics of enriched bacteria at the class level. *Deltaproteobacteria* (28.26%) and *Betaproteobacteria* (21.36%) were the main bacteria identified in the Control group sample. For the GAC group, *Deltaproteobacteria* (26.33%) and *Betaproteobacteria* (25.38%) were also enriched. In the MwCNTs group, the percentage of *Deltaproteobacteria* increased to 45.30% and the percentage of *Betaproteobacteria* decreased to 14.24%. Similarly, in the Graphite group, the percentage of *Deltaproteobacteria* increased to 34.08% and the percentage of *Betaproteobacteria* decreased to 10.25%. Fig. 5C shows the taxonomic characteristics of the bacteria at the genus level. *Desulfovibrio*, *Syntrophus* and uncultured bacteria were the three most enriched bacteria in the four groups, with the similar percentages. These enriched bacteria were different from that in the raw sludge sample in which Family_XIV_uncultured, *Atribacteria*_norank, and *Gelria*

Table 4
Taxonomic affiliation and percentages of archaeal community sequences.

Affliction		Percentage of archaeal sequences (%)			
Class	Genus	Control	GAC	MwCNTs	Graphite
Methanomicrobia		0.13	0.12	0.15	0.16
	Methanoculleus	0.10	0.08	0.13	0.14
	Methanosarcina	0.03	0.04	0.02	0.02

were the three main bacteria. In the GAC group, the percentage of *Azonexus* was 18.20%, but this percentage was below 1% in the other three groups. *Syntrophus* is a benzoate-degrading genera that can associate with syntrophs such as *Desulfovibrio* strain G11 (Jackson et al., 1999). Cervantes et al. (2002) reported that humus can serve as a terminal electron acceptor to support the growth of *Desulfovibrio* G11 using H_2 and lactate as substrates. In this study, *Desulfovibrio* was also enriched.

The percentage of archaea was rather low (<0.5%), and Table 4 summarizes the changes of archaeal communities in detail. The identified archaea belonged to *Methanomicrobia* at the class level, and the percentages in Control, GAC, MwCNTs, and Graphite groups were 0.13%, 0.12%, 0.15%, and 0.16%, respectively. *Methanoculleus* and *Methanosarcina* were the two main archaea at the genus level. The *Methanoculleus* percentages in the four groups were 0.10%, 0.08%, 0.13%, and 0.14%, respectively. The *Methanosarcina* percentages in the four groups were lower, 0.03%, 0.04%, 0.02% and 0.02%, respectively. *Methanoculleus* is a hydrogenotrophic methanogen that can convert H_2/CO_2 to CH_4 (Thauer et al., 2008). *Methanosarcina* is more metabolically versatile, and can use the substrates of both H_2/CO_2 and acetate to produce methane (De Vrieze et al., 2012). Rotaru et al. (2014) also reported that DIET occurred between *Geobacter metallireducens* and *Methanosarcina barkeri*. Thus, *Methanosarcina* can also accept electrons from *Desulfovibrio* by DIET, but, it shall also be verified in the future.

Zhuang et al. (2015) studied benzoate degradation by adding hematite and magnetite, and reported activity through both DIET (*proteobacteria* and *Methanobacterium*) and the syntrophic acetate-oxidizing and hydrogenotrophic methanogen pathway (SAO-HM, *Clostridia* and *Methanobacterium*) for the conversion of acetate to methane. Thus, based on the sequencing results, the benzoate degrading process is proposed as shown in Fig. 6. In this pathway, benzoate is degraded by *Syntrophus* to acetate and H_2. Three pathways were proposed to convert acetate to methane via: i) AM, acetoclastic methanogens of *Methanosarcina*; ii) SAO-HM, syntrophic acetate-oxidizing bacteria (*Clostridia*) and hydrogenotrophic methanogens of *Methanoculleus* and *Methanosarcina*; and iii) DIET of *proteobacteria* and *Methanosarcina*. H_2 was converted to methane via two pathways, i) HM, hydrogenotrophic methanogens of *Methanoculleus* and *Methanosarcina*; and ii) DIET of *Desulfovibrio* and *Methanosarcina*. This proposed benzoate degrading process is consistent with the results in Figs. 1 and 2. However, Li et al. (2018) reported that carbon cloth obviously promoted acetoclastic methanogenesis via *Methanosarcina* instead of CO_2 reduction. Thus, the role of *Methanosarcina* shall also be verified in the future. Salvador et al. (2017) reported that MwCNTs provided an available surface for microorganism's attachment and nutrients adsorption during butyrate degrading. Thus, other methods including metagenome, metatranscriptome and electrochemical analysis shall also be carried out to reveal the mechanism in the future.

3.4. Benzoate degradation by addition of carbon materials

Benzoate is a key product in anaerobic degradation of phenol and many complex aromatic chemicals, making it a common pollutant in wastewater from chemical industries (Upadhyay et al., 2008). Acetate and H_2 are two intermediates in the syntrophic benzoate degradation process, thus the thermodynamics of Eq. (1) are strongly influenced by acetate concentrations or H_2 partial pressure (Varjani, 2017). Upadhyay et al. (2008) reported that only 60–80% of benzoate was consumed in a UASB reactor even after 20 days, which was longer than that of present study (15 days). In this work, addition of carbon materials could stimulate electron transfer, explaining why H_2 was undetected and benzoate was totally consumed.

Acetate was accumulated as a result of adding carbon materials during the degradation of benzoate. The inward diffusion of organic acids leads to dissipation of produced ATP in anaerobic bacteria (Hackmann et al., 2013). Thus, acetate accumulation may reduce the activity of both benzoate-degrading bacteria and methanogens. Jiang et al. (2011) constructed a fibrous bed bioreactor (FBB) to immobilize *Clostridium tyrobutyricum* to enhance the production of butyric acid (amount to 86.9 g/L). In the present study, the maximum concentration of acetate in the Control group in the second cycle (28.7 mM) was much higher than that of other groups. Thus, the biofilm formed on carbon materials reduces the toxicity of acetate. Recently, Dai et al. (2019) reported the removal of organic acids from the broth by electrodialysis to improve the performance of methanogens. Thus, acetate removal

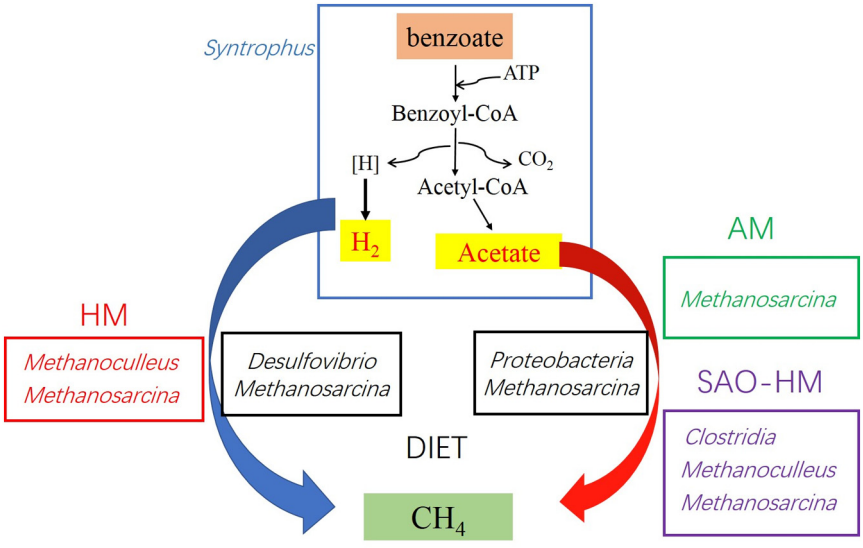

Fig. 6. Proposed process of benzoate degradation.

coupled with carbon addition would be an effective strategy for improved benzoate dageradation and acetate recovery, however, much more works such as the effect of acetate on the degradation of benzoate shall also be carried out to demonstrate the role of conductive carbon materials.

AD is an important biotechnology to convert organic wastes (i.e., activated sludge or organic wastewater) to biogas (Krishnan et al., 2019; Massaro et al., 2015; Zhang et al., 2019). Moreover, the International Renewable Energy Agency demonstrated that in 2015, the worldwide produced bioenergy such as biogas accounted for around 10% of whole energy consumption (Dai et al., 2020). Recently, Zhao et al. (2017) reported that DIET offered the potential to enhance anaerobic digestion of complex organic waste. Morita et al. (2011) also reported that DIET occurred within microbial aggregates derived from a UASB reactor converting brewery waste to methane. Besides GAC, biochar is another interesting material in DIET (Chen et al., 2014), and Liu et al. (2017) demonstrated that biochar provided benefits of stable microorganism community structure and served as an electron shuttle. Thus, conductive carbon materials stimulating methanogenic degradation of benzoate should be next assessed in pilot-scale reactors.

4. Conclusions

Conductive carbon minerals of GAC, MwCNTs, and graphite stimulated the methanogenic degradation of benzoate. The measured benzoate-degrading rates were in the sequence of GAC (5 g/L) > MwCNTs (1 g/L) ~ Graphite (100 mg/L) > Control. A total of 82–93% of the electrons released from added benzoate were recovered. Acetate was the sole carbon-bearing intermediate of benzoate by enriched anaerobic bacteria. Taxonomic analyses revealed that benzoate was degraded by *Syntrophus* to acetate and H_2, which were further converted to methane by *Methanosarcina* (acetoclastic methanogens), *Methanoculleus* and *Methanosarcina* (hydrogenotrophic methanogens), and DIET of *Desulfovibrio* and *Methanosarcina*.

CRediT authorship contribution statement

Fang Zhang: Conceptualization, Writing - review & editing, Methodology, Formal analysis, Writing - original draft. **Ding-Kang Qian:** Methodology, Writing - review & editing. **Xian-Bin Wang:** Methodology, Writing - review & editing, Formal analysis, Writing - original draft. **Kun Dai:** Formal analysis, Writing - review & editing. **Ting Wang:** Methodology, Writing - review & editing. **Wei Zhang:** Formal analysis, Writing - review & editing. **Raymond Jianxiong Zeng:** Conceptualization, Writing - review & editing, Formal analysis, Writing - original draft.

Declaration of competing interest

The authors declare that they have no known competing financial interests or personal relationships that could have appeared to influence the work reported in this paper.

Acknowledgements

The authors would like to acknowledge the financial support from the National Key Research and Development Program of China (2018YFE0107000), the National Natural Science Foundation of China (Grant no: 51878175 and 51808120), and the Program for Innovative Research Team in Science and Technology in Fujian Province University (IRTSTFJ).

Appendix A. Supplementary data

Supplementary data to this article can be found online at https://doi.org/10.1016/j.scitotenv.2020.138080.

References

Aburto-Medina, A., Ball, A.S., 2015. Microorganisms involved in anaerobic benzene degradation. Ann. Microbiol. 65 (3), 1201–1213.
Cervantes, F.J., Bok, F.A.M.d., Duong-Dac, T., Stams, A.J.M., Lettinga, G., Field, J.A., 2002. Reduction of humic substances by halorespiring, sulphate-reducing and methanogenic microorganisms. Environ. Microbiol. 4 (1), 51–57.
Chen, S., Rotaru, A.E., Shrestha, P.M., Malvankar, N.S., Liu, F., Fan, W., Nevin, K.P., Lovley, D.R., 2014. Promoting interspecies electron transfer with biochar. Sci. Rep. 4, 5019.
Chen, Y., Zhang, F., Wang, T., Shen, N., Yu, Z.-W., Zeng, R.J., 2016. Hydraulic retention time affects stable acetate production from tofu processing wastewater in extreme-thermophilic (70 °C) mixed culture fermentation. Bioresour. Technol. 216, 722–728.
Dai, K., Wen, J.-L., Zhang, F., Zeng, R.J., 2017. Valuable biochemical production in mixed culture fermentation: fundamentals and process coupling. Appl. Microbiol. Biotechnol. 101 (17), 6575–6586.
Dai, K., Wen, J.-L., Wang, Y.-L., Wu, Z.-G., Zhao, P.-J., Zhang, H.-H., Wang, J.-J., Zeng, R.J., Zhang, F., 2019. Impacts of medium composition and applied current on recovery of volatile fatty acids during coupling of electrodialysis with an anaerobic digester. J. Clean. Prod. 207, 483–489.
Dai, K., Zhang, W., Zeng, R.J., Zhang, F., 2020. Production of chemicals in thermophilic mixed culture fermentation: mechanism and strategy. Crit. Rev. Environ. Sci. Technol. 50 (1), 1–30.
De Vrieze, J., Hennebel, T., Boon, N., Verstraete, W., 2012. Methanosarcina: the rediscovered methanogen for heavy duty biomethanation. Bioresour. Technol. 112 (0), 1–9.
Fuchs, G., Boll, M., Heider, J., 2011. Microbial degradation of aromatic compounds — from one strategy to four. Nat. Rev. Microbiol. 9 (11), 803–816.
Ghattas, A.-K., Fischer, F., Wick, A., Ternes, T.A., 2017. Anaerobic biodegradation of (emerging) organic contaminants in the aquatic environment. Water Res. 116, 268–295.
Guo, X.J., Lu, Z.Y., Wang, P., Li, H., Huang, Z.Z., Lin, K.F., Liu, Y.D., 2015. Diversity and degradation mechanism of an anaerobic bacterial community treating phenolic wastewater with sulfate as an electron acceptor. Environ. Sci. Pollut. Res. 22 (20), 16121–16132.
Hackmann, T.J., Diese, L.E., Firkins, J.L., 2013. Quantifying the responses of mixed rumen microbes to excess carbohydrate. Appl. Environ. Microbiol. 79 (12), 3786–3795.
Jackson, B.E., Bhupathiraju, V.K., Tanner, R.S., Woese, C.R., McInerney, M.J., 1999. Syntrophus aciditrophicus sp. nov., a new anaerobic bacterium that degrades fatty acids and benzoate in syntrophic association with hydrogen-using microorganisms. Arch. Microbiol. 171 (2), 107–114.
Jiang, L., Wang, J., Liang, S., Cai, J., Xu, Z., Cen, P., Yang, S., Li, S., 2011. Enhanced butyric acid tolerance and bioproduction by Clostridium tyrobutyricum immobilized in a fibrous bed bioreactor. Biotechnol. Bioeng. 108 (1), 31–40.
Jin, Z., Zhao, Z., Zhang, Y., 2019. Potential of direct interspecies electron transfer in synergetic enhancement of methanogenesis and sulfate removal in an up-flow anaerobic sludge blanket reactor with magnetite. Sci. Total Environ. 677, 299–306.
Krishnan, S., Md Din, M.F., Taib, S.M., Nasrullah, M., Sakinah, M., Wahid, Z.A., Kamyab, H., Chelliapan, S., Rezania, S., Singh, L., 2019. Accelerated two-stage bioprocess for hydrogen and methane production from palm oil mill effluent using continuous stirred tank reactor and microbial electrolysis cell. J. Clean. Prod. 229, 84–93.
Li, J., Xiao, L., Zheng, S., Zhang, Y., Luo, M., Tong, C., Xu, H., Tan, Y., Liu, J., Wang, O., Liu, F., 2018. A new insight into the strategy for methane production affected by conductive carbon cloth in wetland soil: beneficial to acetoclastic methanogenesis instead of CO2 reduction. Sci. Total Environ. 643, 1024–1030.
Li, X., Li, Y., Zhang, X., Zhao, X., Sun, Y., Weng, L., Li, Y., 2019. Long-term effect of biochar amendment on the biodegradation of petroleum hydrocarbons in soil microbial fuel cells. Sci. Total Environ. 651, 796–806.
Liu, Y., He, P., Shao, L., Zhang, H., Lü, F., 2017. Significant enhancement by biochar of caproate production via chain elongation. Water Res. 119, 150–159.
Martins, G., Salvador, A.F., Pereira, L., Alves, M.M., 2018. Methane production and conductive materials: a critical review. Environmental Science & Technology 52 (18), 10241–10253.
Massaro, V., Digiesi, S., Mossa, G., Ranieri, L., 2015. The sustainability of anaerobic digestion plants: a win–win strategy for public and private bodies. J. Clean. Prod. 104, 445–459.
Morita, M., Malvankar, N.S., Franks, A.E., Summers, Z.M., Giloteaux, L., Rotaru, A.E., Rotaru, C., Lovley, D.R., 2011. Potential for direct interspecies electron transfer in methanogenic wastewater digester aggregates. mBio 2 (4) (e00159-11).
Morris, B.E.L., Henneberger, R., Huber, H., Moissl-Eichinger, C., 2013. Microbial syntrophy: interaction for the common good. FEMS Microbiol. Rev. 37 (3), 384–406.
Mrozik, A., Piotrowska-Seget, Z., 2010. Bioaugmentation as a strategy for cleaning up of soils contaminated with aromatic compounds. Microbiol. Res. 165 (5), 363–375.
Nobu, M.K., Narihiro, T., Liu, M., Kuroda, K., Mei, R., Liu, W.-T., 2017. Thermodynamically diverse syntrophic aromatic compound catabolism. Environ. Microbiol. 19 (11), 4576–4586.
Pathiraja, G., Egodawatta, P., Goonetilleke, A., Te'o, V.S.J., 2019. Effective degradation of polychlorinated biphenyls by a facultative anaerobic bacterial consortium using alternating anaerobic aerobic treatments. Sci. Total Environ. 659, 507–514.
Rotaru, A.-E., Shrestha, P.M., Liu, F., Markovaite, B., Chen, S., Nevin, K.P., Lovley, D.R., 2014. Direct interspecies electron transfer between Geobacter metallireducens and Methanosarcina barkeri. Appl. Environ. Microbiol. 80 (15), 4599.
Salvador, A.F., Martins, G., Melle-Franco, M., Serpa, R., Stams, A.J.M., Cavaleiro, A.J., Pereira, M.A., Alves, M.M., 2017. Carbon nanotubes accelerate methane production in pure cultures of methanogens and in a syntrophic coculture. Environ. Microbiol. 19 (7), 2727–2739.

Shrestha, P.M., Rotaru, A.-E., 2014. Plugging in or going wireless: strategies for interspecies electron transfer. Front. Microbiol. 5, 237.
Singh, P., Jain, R., Srivastava, N., Borthakur, A., Pal, D.B., Singh, R., Madhav, S., Srivastava, P., Tiwary, D., Mishra, P.K., 2017. Current and emerging trends in bioremediation of petrochemical waste: a review. Crit. Rev. Environ. Sci. Technol. 47 (3), 155–201.
Tabassum, M.R., Xia, A., Murphy, J.D., 2017. Comparison of pre-treatments to reduce salinity and enhance biomethane yields of Laminaria digitata harvested in different seasons. Energy 140, 546–551.
Thauer, R.K., Kaster, A.K., Seedorf, H., Buckel, W., Hedderich, R., 2008. Methanogenic archaea: ecologically relevant differences in energy conservation. Nat. Rev. Microbiol. 6 (8), 579–591.
Upadhyay, U., Kumar, P., Mehrotra, I., 2008. Anaerobic degradation of benzoate: batch studies. Bioresour. Technol. 99 (15), 6861–6865.
Varjani, S.J., 2017. Microbial degradation of petroleum hydrocarbons. Bioresour. Technol. 223, 277–286.
Venkidusamy, K., Megharaj, M., Marzorati, M., Lockington, R., Naidu, R., 2016. Enhanced removal of petroleum hydrocarbons using a bioelectrochemical remediation system with pre-cultured anodes. Sci. Total Environ. 539, 61–69.
Vogt, C., Kleinsteuber, S., Richnow, H.-H., 2011. Anaerobic benzene degradation by bacteria. Microb. Biotechnol. 4 (6), 710–724.
Wang, H.-J., Dai, K., Xia, X.-Y., Wang, Y.-Q., Zeng, R.J., Zhang, F., 2018. Tunable production of ethanol and acetate from synthesis gas by mesophilic mixed culture fermentation in a hollow fiber membrane biofilm reactor. J. Clean. Prod. 187, 165–170.
Xiao, L., Liu, F., Liu, J., Li, J., Zhang, Y., Yu, J., Wang, O., 2018. Nano-Fe3O4 particles accelerating electromethanogenesis on an hour-long timescale in wetland soil. Environmental Science: Nano 5 (2), 436–445.
Xiao, L., Sun, R., Zhang, P., Zheng, S., Tan, Y., Li, J., Zhang, Y., Liu, F., 2019. Simultaneous intensification of direct acetate cleavage and CO2 reduction to generate methane by bioaugmentation and increased electron transfer. Chem. Eng. J. 378, 122229.
Zhang, F., Zhang, Y., Ding, J., Dai, K., van Loosdrecht, M.C.M., Zeng, R.J., 2014. Stable acetate production in extreme-thermophilic (70°C) mixed culture fermentation by selective enrichment of hydrogenotrophic methanogens. Sci. Rep. 4, 5268.
Zhang, F., Zhang, Y., Chen, Y., Dai, K., van Loosdrecht, M.C.M., Zeng, R.J., 2015. Simultaneous production of acetate and methane from glycerol by selective enrichment of hydrogenotrophic methanogens in extreme-thermophilic (70 degrees C) mixed culture fermentation. Appl. Energy 148, 326–333.
Zhang, W., Dai, K., Xia, X.-Y., Wang, H.-J., Chen, Y., Lu, Y.-Z., Zhang, F., Zeng, R.J., 2018. Free acetic acid as the key factor for the inhibition of hydrogenotrophic methanogenesis in mesophilic mixed culture fermentation. Bioresour. Technol. 264, 17–23.
Zhang, F., Zhang, W., Qian, D.-K., Dai, K., van Loosdrecht, M.C.M., Zeng, R.J., 2019. Synergetic alginate conversion by a microbial consortium of hydrolytic bacteria and methanogens. Water Res. 163, 114892.
Zhao, Z., Li, Y., Quan, X., Zhang, Y., 2017. Towards engineering application: potential mechanism for enhancing anaerobic digestion of complex organic waste with different types of conductive materials. Water Res. 115, 266–277.
Zhuang, L., Tang, J., Wang, Y., Hu, M., Zhou, S., 2015. Conductive iron oxide minerals accelerate syntrophic cooperation in methanogenic benzoate degradation. J. Hazard. Mater. 293, 37–45.